JACC: CARDIOVASCULAR IMAGING
VOL. 10, NO. 6, 2017

ISSN 1936-878X/$36.00
PUBLISHED BY ELSEVIER
http://dx.doi.org/10.1016/j.jcmg.2016.04.012

Impact of Longitudinal Lesion Geometry on Location of Plaque Rupture and Clinical Presentations

Joo Myung Lee, MD, MPH, PhD,[a] Gilwoo Choi, PhD,[b,c] Doyeon Hwang, MD,[d] Jonghanne Park, MD, PhD,[d] Hyun Jin Kim, PhD,[b] Joon-Hyung Doh, MD, PhD,[e] Chang-Wook Nam, MD, PhD,[f] Sang-Hoon Na, MD, PhD,[g,h] Eun-Seok Shin, MD, PhD,[i] Charles A. Taylor, PhD,[b,j] Bon-Kwon Koo, MD, PhD[d,h]

ABSTRACT

OBJECTIVES This study sought to investigate the impact of longitudinal lesion geometry on the location of plaque rupture and clinical presentation and its mechanism.

BACKGROUND The relationships among lesion geometry, external hemodynamic forces acting on the plaque, location of plaque rupture, and clinical presentation have not been comprehensively investigated.

METHODS This study enrolled 125 patients with plaque rupture documented by intravascular ultrasound. Longitudinal locations of plaque rupture were identified and categorized by intravascular ultrasound. Patients' clinical presentations and TIMI (Thrombolysis In Myocardial Infarction) flow grade in an initial angiogram were compared according to the location of plaque rupture. Longitudinal lesion asymmetry was quantitatively assessed by the luminal radius change over the segment length (radius gradient [RG]). Lesions with a steeper radius change in the upstream segment compared with the downstream segment ($RG_{upstream} > RG_{downstream}$) were defined as upstream-dominant lesions.

RESULTS On the basis of the site of maximum rupture aperture, 56.0%, 16.0%, and 28.0% of the patients had upstream, minimal lumen area, and downstream rupture, respectively. Patients with upstream rupture more frequently presented with ST-segment elevation myocardial infarction (45.7%, 40.0%, 22.9%; $p = 0.030$) and with TIMI flow grade <3 (32.9%, 20.0%, 17.1%; $p = 0.042$). According to the ratio of upstream and downstream RG, 69.5% of lesions were classified as upstream-dominant lesions, and 30.5% were classified as downstream-dominant lesions. Among the 66 upstream-dominant lesions, 65 cases (98.5%) had upstream rupture, and the RG ratio ($RG_{upstream}/RG_{downstream}$) was an independent predictor of upstream rupture (odds ratio: 1.481; 95% confidence interval: 1.035 to 2.120; $p = 0.032$). Upstream-dominant lesions more frequently manifested with ST-segment elevation myocardial infarction than did downstream-dominant lesions (48.5% vs. 24.1%; $p = 0.026$).

CONCLUSIONS Both clinical presentation and degree of flow limitation were associated with the location of plaque rupture. Longitudinal lesion asymmetry assessed by RG, which can affect regional distribution of hemodynamic stress, was associated with the location of rupture and with clinical presentation. (J Am Coll Cardiol Img 2017;10:677–88)

From the [a]Division of Cardiology, Department of Internal Medicine, Heart Vascular Stroke Institute, Samsung Medical Center, Sungkyunkwan University School of Medicine, Seoul, South Korea; [b]HeartFlow, Inc., Redwood City, California; [c]Department of Surgery, Stanford University Medical Center, Stanford, California; [d]Department of Medicine, Seoul National University Hospital, Seoul, South Korea; [e]Department of Medicine, Inje University Ilsan Paik Hospital, Goyang, South Korea; [f]Department of Medicine, Keimyung University Dongsan Medical Center, Daegu, South Korea; [g]Department of Internal Medicine and Emergency Medical Center, Seoul National University Hospital, Seoul, South Korea; [h]Institute of Aging, Seoul National University, Seoul, South Korea; [i]Department of Cardiology, Ulsan University Hospital, University of Ulsan College of Medicine, Ulsan, South Korea; and the [j]Department of Bioengineering, Stanford University, Stanford, California. Drs. Choi, Kim, and Taylor are employees and shareholders of HeartFlow. All other authors have reported that they have no relationships relevant to the contents of this paper to disclose.

Manuscript received February 19, 2016; accepted April 16, 2016.

ABBREVIATIONS AND ACRONYMS

APS = axial plaque stress

CFD = computational fluid dynamics

IVUS = intravascular ultrasound

MLA = minimal lumen area

RG = radius gradient

STEMI = ST-segment elevation myocardial infarction

Although coronary plaque rupture is the main pathophysiological trigger for acute coronary syndrome, previous studies have shown that not all ruptured plaques cause clinically significant flow limitation or acute coronary syndrome (1). Several studies have explored longitudinal or circumferential rupture location and its relationship with clinical presentation (1,2) or have characterized morphological features of ruptured plaque according to different clinical presentations (3-6). However, the possible mechanistic explanations for the specific rupture location and its clinical presentation have not been fully investigated.

SEE PAGE 689

Plaque rupture is related in a complex manner to intrinsic properties of individual plaque (vulnerability), extrinsic forces on plaque (trigger force), and strain within the plaque. The lesion geometry determines the distribution of hemodynamic forces that can act as a trigger force for plaque rupture and influence the nature and constituents of the plaque itself (7). Therefore, assessment of lesion geometry may be helpful to understand the mechanism of rupture. Our group previously demonstrated the relationship between axial plaque stress (APS), one of the major hemodynamic stresses acting on plaque, and lesion geometry using patient-specific computational fluid dynamics (CFD) models using coronary computed tomography (CT) angiography (8).

In this study, we sought to evaluate the impact of longitudinal lesion geometry on the location of plaque rupture and clinical presentations by using intravascular ultrasound (IVUS) data. In addition, we explored the possible mechanistic link between longitudinal lesion geometry and rupture locations by using CFD and idealized models created from IVUS data.

METHODS

PATIENT POPULATION. Between February 2009 and May 2014, 174 consecutive patients with ruptured plaque as determined by IVUS were selected from 4 university hospitals in South Korea. Among these, 49 patients (28.2%) were excluded from the final analysis, as presented in **Figure 1**. Briefly, we excluded lesions with the following characteristics: 1) multiple ruptures (e.g., rupture cavities were observed both in upstream and downstream segments); 2) ostial location of ruptured plaque; 3) ruptured plaque within the previously implanted stent; 4) diffuse atherosclerotic involvement with lesion length >30 mm; 5) equivocal evidence of plaque rupture; or 6) catheter-induced plaque rupture. The remaining 125 patients with definitive evidence of plaque rupture as shown by IVUS were included in this study. The study protocol was approved by the ethics committee of each site and was in accordance with the Declaration of Helsinki.

CORONARY ANGIOGRAPHY. Selective invasive coronary angiography was performed using standard techniques. All angiograms were obtained after intracoronary bolus injection of 100 to 200 μg of nitroglycerin. All angiograms were reviewed at a core laboratory (Seoul National University Hospital, Seoul, South Korea) by 2 independent observers (J.M.L and J.P.) who were unaware of the IVUS findings in a blinded fashion. Flow limitation in the vessel with ruptured plaque was assessed with TIMI (Thrombolysis in Myocardial Infarction) criteria on initial angiography (9).

ACQUISITION OF IVUS IMAGE AND DATA ANALYSIS. IVUS images were obtained after intracoronary administration of 200 μg of nitroglycerin using commercially available systems. In case of total occlusion, IVUS was performed after thrombosuction. Images were acquired with automated pullback at 0.5 mm/s. IVUS images were analyzed using commercially available software (echoPlaque 4.0, INDEC Medical Systems, Santa Clara, California) at a core laboratory in a blinded fashion. The locations of rupture were assessed by 2 independent observers (D.H. and Dong-Jun Lee) who were unaware of angiographic findings and clinical information. The ruptured plaque was defined by IVUS as a plaque containing a cavity that communicated with the lumen with or without overlying residual fibrous cap fragments or plaques (1,2).

The longitudinal location of plaque rupture was classified using the following criteria (**Figure 2**):

- Upstream rupture: The center of maximum aperture of the ruptured plaque is located between the proximal edge and the minimal lumen area (MLA) site of plaque (**Figure 2A**).
- MLA rupture: The center of maximum aperture of the ruptured plaque is located at the center of plaque; therefore, the MLA site could not be precisely marked in the IVUS image (**Figure 2B**).
- Downstream rupture: The center of maximum aperture of the ruptured plaque is located between the distal edge and the MLA site of plaque (**Figure 2C**).

Evaluation of 2- and 3-dimensional lesion morphological features and other measurements of IVUS images were performed according to the American College of Cardiology Clinical Expert Consensus Document on Standards for Acquisition, Measurement, and Reporting of Intravascular Ultrasound

FIGURE 1 Study Flow

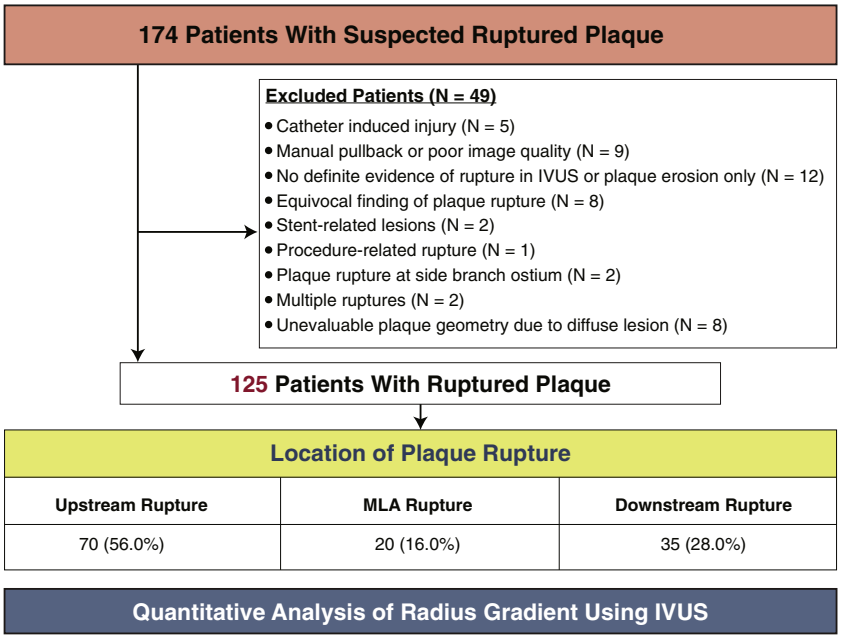

Study flow and reasons for exclusion are presented. The 125 ruptured plaques were classified as upstream, minimum lumen area (MLA), or downstream rupture, according to the location of maximum aperture. IVUS = intravascular ultrasound.

FIGURE 2 Representative Cases of Longitudinal Location of Plaque Rupture

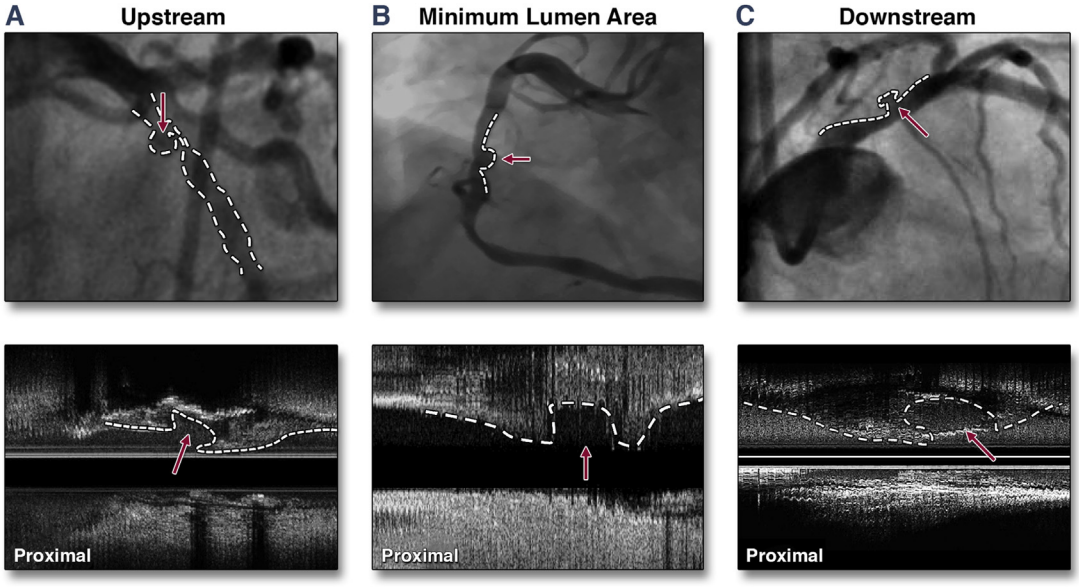

(A to C) Representative cases of upstream, minimum lumen area, and downstream ruptured plaque are presented. The **red arrows** indicate the maximum aperture in the ruptured plaque.

Studies (1,10). Measured quantitative IVUS parameters included external elastic membrane (EEM) area, lumen cross-sectional area (CSA), MLA, plaque plus media (P+M) area, and upstream and downstream segmental lesion length. Plaque burden was calculated as follows: [(P+M CSA) / (EEM CSA)] × 100. The remodeling index was calculated as follows: (EEM CSA at the MLA site) / (average of the proximal and distal reference EEM CSA). The reference site was the frame showing the largest lumen area and smallest plaque burden within 5 mm proximally and distally from the target segment (10). The start and endpoints of the target segment were defined as points of 50% plaque burden.

Among several hemodynamic forces acting on the plaque, APS has been regarded as the main mechanical force in clinically relevant stenoses (11–13), and the shape of upstream and downstream segments of the stenosis affects the direction and magnitude of the axial hemodynamic force acting on the plaque. Previously, we devised a geometric descriptor, radius gradient (RG), to describe the axial (i.e., longitudinal) geometric change of the stenosis quantitatively (8). Briefly, RG was defined by the change in radius over the segmental lesion length, where radius change refers to the difference between the lesion starting-point (or ending-point) radius and the radius at the location of MLA. Segmental lesion length was defined by the length from the lesion starting point (or ending point) to MLA location. Because APS can be expressed as a function of pressure and RG, RG can be used as a quantitative geometric descriptor and a surrogate marker of APS. The relationship between APS and RG is presented in Online Figure 1 (8).

For the RG calculation, proximal starting points and distal ending points were defined as being 2 mm inward from the edge of a target segment, to avoid systemic bias from progressive widening of lumen area from distal to proximal portion of vessels. Cases of MLA rupture were excluded from RG measurement. RG was calculated by 2 independent observers, and reliability testing was performed to confirm reproducibility of this quantitative measure. The 2 RG measurements between 2 independent observers showed good reproducibility and interobserver agreement (Online Figure 2). Lesions with steeper radius change in upstream compared with downstream segments ($RG_{upstream} > RG_{downstream}$) were defined as "upstream-dominant lesions," whereas lesions with steeper radius change in downstream compared with upstream segments ($RG_{upstream} < RG_{downstream}$) were defined as "downstream-dominant lesions."

IDEALIZED STENOSIS MODEL AND COMPUTATIONAL FLUID DYNAMICS ANALYSIS. To provide an intuitive and simplified explanation of the mechanistic link between lesion geometry and distribution of APS, CFD analysis was performed. Idealized stenosis models were constructed using average values of IVUS measurements of the study population. From CFD analysis, APS was computed in each segment of the stenosis lesion, as previously described (8,14).

STATISTICAL ANALYSIS. Categorical variables were given as counts and percentages, and continuous variables were described as mean ± SD or median and interquartile range as appropriate. Comparison of categorical variables among patients classified according to rupture locations was performed with the chi-square test. Comparison of normally distributed continuous variables among the 3 groups was performed with the one-way analysis of variance test. For comparison of IVUS data between upstream and downstream ruptured plaques, an independent Student *t* test or Mann-Whitney *U* test was used, according to their distribution and homogeneity of the variance. The comparison of segmental RG between upstream and downstream segments in one lesion was performed with a paired-sample *t* test or Wilcoxon signed rank sum test. The intraclass correlation coefficient was used to assess the reliability and agreement between the 2 measurements of RG.

To explore the independent predictors for upstream rupture, TIMI flow grade <3, or ST-segment elevation myocardial infarction (STEMI), 3 independent multivariate logistic regression models were constructed. The covariates used in each multivariate logistic regression model were selected if they were significantly different between the 2 groups ($p < 0.1$) or if they were clinically relevant. The discriminant function of the model was presented with a c-index and 95% confidence interval (CI). All probability values were 2 sided, and p values <0.05 were considered statistically significant. The statistical package SPSS version 18.0 (SPSS Inc., Chicago, Illinois) and R programming language version 3.1.3 (R Foundation for Statistical Computing, Vienna, Austria) were used for statistical analyses.

RESULTS

PATIENTS' CHARACTERISTICS AND CLINICAL PRESENTATIONS ACCORDING TO RUPTURE LOCATION. On the basis of the site of maximum aperture longitudinally, the patients were divided into 3 groups as follows: upstream rupture (n = 70; 56.0%); MLA rupture (n = 20; 16.0%); and downstream rupture (n = 35; 28.0%). Patients' characteristics according to rupture location are summarized in Table 1. The frequencies of acute myocardial infarction (AMI), including acute STEMI, and non-STEMI versus non-AMI were significantly

different according to rupture locations (p = 0.042). In patients with upstream rupture, 65.7% presented with AMI and 34.3% with conditions other than AMI. Conversely, patients with lesions with downstream rupture showed an opposite trend (AMI, 40.0%; conditions other than AMI, 60.0%) (Figure 3). STEMI was also more frequently observed in patients with lesions with upstream ruptures than with MLA or downstream ruptures (Table 1). In a multivariate model, independent predictors of STEMI were the presence of an upstream rupture (odds ratio [OR]: 3.943; 95% CI: 1.341 to 11.593; p = 0.013), current smoking (OR: 3.379; 95% CI: 1.125 to 10.148; p = 0.030), plaque burden (OR: 1.248; 95% CI: 1.081 to 1.440; p = 0.003), and lesion length (OR: 0.907; 95% CI: 0.838 to 0.982; p = 0.016) (Online Table 1).

ANGIOGRAPHIC AND INTRAVASCULAR ULTRASOUND FINDINGS ACCORDING TO RUPTURE LOCATIONS. Angiographic characteristics are presented in Table 2. The right coronary artery showed a relatively higher incidence of MLA rupture than the other coronary arteries. The frequency of TIMI flow grade 0 (17.1%, 5.0%, and 5.7% for upstream, MLA, and downstream rupture, respectively) or TIMI flow grade <3 on initial angiogram (32.9%, 25.0%, and 14.3%, respectively; p = 0.042) was significantly higher in patients with lesions with upstream rupture (Table 2). The presence of an upstream rupture was an independent predictor of TIMI flow grade <3 (OR: 2.932; 95% CI: 1.014 to 8.475; p = 0.047). In addition, plaque burden (OR: 1.226; 95% CI: 1.050 to 1.432; p = 0.010) and lesion length (OR: 0.915; 95% CI: 0.837 to 0.999; p = 0.048) were also independent predictors of TIMI flow grade <3 (Online Table 1).

Pre-interventional IVUS findings are summarized in Table 3. There were no significant differences regarding stenosis severity, remodeling index, incidence of posterior attenuating plaque, or plaque burden between the upstream and downstream ruptured plaques.

ASSOCIATION BETWEEN LONGITUDINAL LESION ASYMMETRY AND RUPTURE LOCATION. A total of 95 ruptured plaques were included in RG measurement; 66 cases were classified as upstream-dominant lesions (69.5%), and 29 cases were classified as downstream-dominant lesions (30.5%), according to longitudinal asymmetry of lesion geometry. Among the 66 upstream-dominant lesions, 65 cases (98.5%) showed upstream rupture; conversely, all 29 downstream-dominant lesions showed downstream rupture (p < 0.001). In a comparison of RG between upstream and downstream segments according to rupture location, the upstream RG was significantly higher than the downstream RG in lesions with upstream rupture. Conversely, in the lesions with downstream rupture, the RGs of the downstream segment were significantly higher than those of the upstream segment (Table 4, Figure 4). The significant association between longitudinal lesion asymmetry and rupture location was also supported by the results of a multivariate logistic regression model. The RG ratio ($RG_{upstream}/RG_{downstream}$) was the only independent predictor of upstream rupture (OR: 1.481; 95% CI: 1.035 to 2.120; p = 0.032) (Online Table 1).

TABLE 1 Clinical Characteristics

	Upstream Rupture	MLA Rupture	Downstream Rupture	p Value
Patients	70 (56.0)	20 (16.0)	35 (28.0)	
Age, yrs	60.7 ± 12.4	65.2 ± 10.9	61.7 ± 13.0	0.369
Male	61 (87.1)	17 (85.0)	26 (74.3)	0.246
Obesity (BMI >25 kg/m^2)	32 (47.8)	10 (52.6)	13 (38.2)	0.537
Systemic hypertension	30 (42.9)	10 (50.0)	18 (51.4)	0.666
Diabetes mellitus	19 (27.1)	6 (30.0)	11 (31.4)	0.893
Hypercholesterolemia	34 (48.6)	12 (60.0)	15 (42.9)	0.472
Current smoking	34 (48.6)	8 (40.0)	15 (42.9)	0.738
Clinical diagnosis				0.030
STEMI (38.4%)	32 (45.7)	8 (40.0)	8 (22.9)	
NSTE-ACS (40.0%)	26 (37.1)	7 (35.0)	17 (48.6)	
NSTEMI	14 (20.0)	3 (15.0)	6 (17.1)	
Unstable angina	12 (17.1)	4 (20.0)	11 (31.4)	
Non-ACS (21.6%)	12 (17.1)	5 (25.0)	10 (28.6)	
Multivessel disease	35 (50.0)	10 (50.0)	21 (60.0)	0.603

Values are n (%) or mean ± SD.

ACS = acute coronary syndrome; BMI = body mass index; MLA = minimum lumen area; NSTE-ACS = non-ST-segment elevation acute coronary syndrome; NSTEMI = non-ST-segment elevation myocardial infarction; STEMI = ST-segment elevation myocardial infarction.

IMPACT OF LESION GEOMETRY ON CLINICAL PRESENTATION AND DEGREE OF FLOW LIMITATIONS. In a comparison of clinical presentation according to the longitudinal asymmetry of lesion geometry, upstream-dominant lesions showed a significantly higher proportion of AMI (69.7% vs. 37.9% for upstream-dominant and downstream-dominant lesions, respectively; p = 0.004) and STEMI (48.5% vs. 24.1%; p = 0.026), compared with downstream-dominant lesions (Figures 5A and 5B). Upstream-dominant lesions showed a relatively higher proportion of TIMI flow grade <3 than downstream-dominant lesions without statistical significance (33.3% vs. 17.2%; p = 0.141).

ASSOCIATION BETWEEN LESION GEOMETRY AND DISTRIBUTION OF HEMODYNAMIC FORCES. Figure 6 demonstrates the distribution of APS according to the longitudinal asymmetry of lesion geometry. The upstream and downstream RGs were 0.108 and 0.059 in upstream-dominant lesions and 0.075 and 0.128 in downstream-dominant lesions, respectively. In upstream-dominant lesions, APS in the upstream segment was higher than in the downstream segment

FIGURE 3 Clinical Presentations According to Rupture Locations

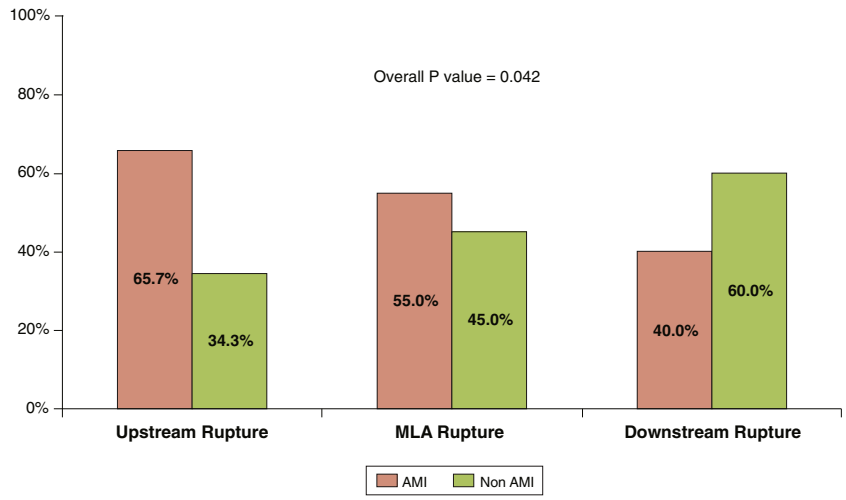

Clinical presentations were significantly different according to the rupture locations. AMI = acute myocardial infarction; MLA = minimum lumen area.

(10,968 dyne/cm^2 vs. 5,651 dyne/cm^2). The inverse was also true for downstream-dominant lesions (7,667 dyne/cm^2 vs. 12,312 dyne/cm^2).

DISCUSSION

The main findings of our study can be summarized as follows. Patients with lesions with upstream rupture showed a higher incidence of STEMI and TIMI flow grade <3 than did those with MLA or downstream rupture. The presence of upstream rupture was an independent predictor of both TIMI flow grade <3 and STEMI. The location of rupture was strongly associated with the longitudinal asymmetry of lesion geometry, which was assessed by RG. In lesions with upstream or downstream segment rupture, the rupture was predominantly located in the segment of higher RG, and the RG ratio ($RG_{upstream}/RG_{downstream}$) was an independent predictor of rupture location. Although plaque rupture results from the complex interactions between various external forces and plaque vulnerability, our results suggest that the assessment of longitudinal lesion asymmetry or RG can be helpful in predicting the location and clinical consequence of plaque rupture.

TABLE 2 Angiographic Characteristics

	Upstream Rupture	MLA Rupture	Downstream Rupture	p Value
Lesions	70 (56.0)	20 (16.0)	35 (28.0)	
Lesion location				0.302
Left main	6 (8.6)	1 (5.0)	5 (14.3)	
LAD	46 (65.7)	11 (55.0)	24 (68.6)	
LCX	4 (5.7)	0 (0.0)	1 (2.9)	
RCA	14 (20.0)	8 (40.0)	5 (14.3)	
Treated with PCI	58 (82.9)	18 (90.0)	30 (85.7)	0.724
TIMI flow grade				0.030
TIMI 0	12 (17.1)	1 (5.0)	2 (5.7)	
TIMI 1	1 (1.4)	0 (0.0)	0 (0.0)	
TIMI 2	10 (14.3)	4 (20.0)	3 (8.6)	
TIMI 3	47 (67.1)	15 (75.0)	30 (85.7)	
TIMI flow grade <3	23 (32.9)	5 (25.0)	5 (14.3)	0.042

Values are n (%).

LAD = left anterior descending coronary artery; LCX = left circumflex coronary artery; MLA = minimum lumen area; PCI = percutaneous coronary intervention; RCA = right coronary artery; TIMI = Thrombolysis in Myocardial Infarction.

Coronary artery plaque rupture is the most detrimental type of plaque-related complication, and it accounts for approximately 70% of cases of fatal AMI or sudden cardiac death (15). Acute coronary syndrome caused by culprit lesions with plaque rupture has been reported to have worse clinical outcomes than when lesions have an intact fibrous cap (16). Therefore, understanding the mechanism of plaque rupture is a pre-requisite to reduce cardiovascular mortality and morbidity. In this regard, several previous studies were performed to clarify various clinical presentations of plaque rupture, "rupture-prone" plaque, and triggering factors for plaque rupture (1,2,6,7,11,15,17). However, clinical research that is focused on the relationship between longitudinal lesion geometry and plaque rupture has been scarce.

ASSOCIATIONS BETWEEN RUPTURE LOCATION AND CLINICAL PRESENTATIONS. In the first part of this

study, we investigated the rupture location and its association with clinical presentation. Similar to results from previous studies of Tanaka et al. (2) and Maehara et al. (1), plaque rupture showed a geographic preponderance. More than one-half of the patients in our cohort had upstream rupture, and more than two-thirds of the ruptures did not involve the MLA site. Fujii et al. (18) also reported the similar trend that plaque rupture did not occur at sites of MLA, but rather at sites of large plaque burden associated with positive remodeling. Tanaka et al. (2) reported that upstream plaque rupture was associated with a higher proportion of TIMI flow grade 0 and was the only independent predictor of STEMI. In our study, patients with upstream rupture more frequently presented with AMI or STEMI, and the frequency of TIMI flow grade <3 was highest in patients with upstream rupture. Moreover, upstream rupture was one of the independent predictors of STEMI. There can be several potential mechanisms to explain the worse clinical presentation and higher incidence of disturbed coronary flow in upstream ruptured plaque. In case of upstream rupture, anterograde blood flow may cause extension of the ruptured cavity, widening of the cavity, and downward displacement of the flap, which lead to more rapid thrombus formation and subsequent distal embolization (2).

IMPACT OF LESION GEOMETRY ON RUPTURE LOCATION, DISTRIBUTION OF HEMODYNAMIC FORCES ACTING ON PLAQUE, AND CLINICAL PRESENTATION. Although atherosclerosis is a systemic process, it remains a geometrically focal disease. Therefore, the geometry of the coronary artery would certainly affect hemodynamic stress distribution, which can influence the microscopic environment or internal strain within the plaque (7,19–21). It is well known that low wall shear stress initiates atherosclerosis, and very high wall shear stress increases the risk of plaque rupture (7,22). Teng et al. (23) investigated the relationship between plaque structural stress and plaque composition assessed by IVUS-virtual histology (VH). Plaque structural stress showed a significant nonlinear relationship with total area and arc of calcification, and total area and arc of necrotic core. In addition, VH-defined thin-cap fibroatheroma had a significantly higher plaque structural stress level than did thick-cap fibrous atheroma. In stenotic lesions, hemodynamic stresses act on both circumferential and axial directions simultaneously. However, as lesion severity increases, the major orientation of maximum principal stress changes direction from circumferential to longitudinal as previously reported by Pagiatakis et al. (12). Because APS can be expressed as a function of pressure and RG, incorporating the concept of RG in the assessment of lesion geometry may be helpful to predict the relative distribution of APS in certain stenotic lesions.

TABLE 3 Pre-Intervention Intravascular Ultrasound Findings for Ruptured Plaques

	Upstream Rupture (n = 70)	Downstream Rupture (n = 35)	p Value
Reference site			
Average lumen area, mm^2	10.15 ± 4.09	9.70 ± 2.90	0.642
Plaque burden, %	44.77 ± 9.27	46.24 ± 8.93	0.554
MLA site			
Lumen area, mm^2	3.06 ± 1.74	3.06 ± 1.45	0.997
Plaque burden, %	83.43 ± 6.92	84.53 ± 5.04	0.443
% area stenosis, %	63.30 ± 13.91	65.79 ± 10.25	0.371
Radius gradient measurement segment			
Segment length, mm	15.54 ± 7.76	12.58 ± 6.43	0.072
Vessel volume index, mm^3/mm	19.98 ± 8.12	23.71 ± 9.33	0.069
Plaque volume index, mm^3/mm	14.26 ± 5.81	16.88 ± 6.10	0.057
Lumen volume index, mm^3/mm	5.85 ± 3.04	7.27 ± 4.04	0.066
Posterior attenuation	28 (48.3)	13 (43.3)	0.888
Remodeling index	1.09 ± 0.19	1.03 ± 0.15	0.166

Values are mean ± SD or n (%).
MLA = minimum lumen area.

Although the relationship between lesion or stenosis geometry and rupture risk was suggested by previous studies (24,25), those studies focused on the degree or pattern of remodeling rather than specific lesion geometry. In this study, we investigated the clinical implication of the geometric descriptor RG in patients with plaque rupture. Longitudinal lesion asymmetry measured with RG showed a significant association with the actual location of plaque rupture. Upstream-dominant lesions mainly showed upstream rupture, whereas downstream-dominant lesions mainly manifested with downstream rupture, and the RG ratio was found to be an independent predictor of upstream rupture. In addition, clinical presentation and degree of flow limitations were also different according to the longitudinal asymmetry of lesion geometry. These results support the previous descriptive studies that described the potential impact of longitudinal asymmetry of lesion geometry on the distribution of hemodynamic stress, a concentration of which is mainly located in plaque shoulders (19,26). CFD analysis also demonstrated that APS was higher in locations with higher RG. This imbalance of APS distribution, according to RG, may represent one of the potential explanations for rupture location and its clinical presentation.

Plaque vulnerability is a well-known major predictor of plaque rupture. The association between plaque vulnerability and acute coronary events was established by post-mortem studies (27), and it has been further validated by several invasive and

TABLE 4 Segmental Analysis of Radius Gradient According to Rupture Location

	Upstream Rupture (Lesion n = 65)			Downstream Rupture (Lesion n = 30)		
	Upstream Segment	Downstream Segment	p Value	Upstream Segment	Downstream Segment	p Value
Segmental length, mm	6.64 ± 3.77	8.90 ± 4.52	<0.001	7.67 ± 5.36	4.92 ± 2.28	0.007
Radius gradient	0.133 (0.070–0.172)	0.063 (0.030–0.095)	<0.001	0.094 (0.057–0.136)	0.132 (0.102–0.173)	<0.001

Values are mean ± SD or median (interquartile range).

noninvasive studies. Plaque vulnerability can be assessed using posterior attenuation, positive remodeling, large plaque burden in IVUS (5,6,28,29), thin-cap fibroatheroma, large lipid pools in optical coherence tomography (30) or IVUS-VH (18,31–33), the napkin ring sign, spot calcification, positive remodeling, or low-attenuation in CT coronary angiography (34,35). Furthermore, a report by Madder et al. (36), using near-infrared spectroscopy, highlighted the importance of maximum lipid core burden index in the development of plaque rupture in STEMI. Nevertheless, because not all vulnerable plaques manifest with acute rupture, integration of plaque geometry, hemodynamic forces acting on plaque, plaque vulnerability, and their interactions would provide comprehensive pathophysiological and clinical insight into plaque rupture. The current study mainly focused on the additional role of lesion geometry and the distribution of hemodynamic forces in plaque rupture. Further study is warranted to clarify the specific role and contribution of each of the foregoing factors in patients with plaque rupture.

MECHANISM AND CLINICAL PRESENTATION OF DOWNSTREAM RUPTURE. Tanaka et al. (2) reported that downstream rupture was found in 36.1% of patients with acute coronary syndrome. In our study, approximately one-third of ruptured plaque lesions showed a maximum aperture located in the downstream segment. Because the direction of blood flow is antegrade, external hemodynamic forces are generally higher in the upstream or MLA segments than in the downstream segment (7,11). However, as presented in the results of idealized models, the magnitude of APS can be greater in downstream segments of downstream-dominant lesions. Our previous study demonstrated that the downstream APS showed a biphasic response to stenosis severity (8).

FIGURE 4 Comparison of RG and Rupture Locations

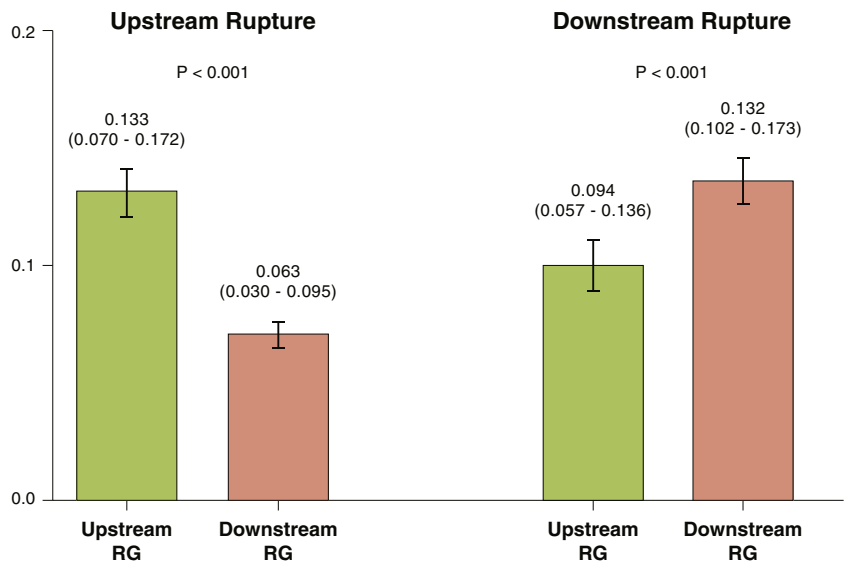

The segmental radius gradient (RG) in upstream or downstream segments was compared according to the rupture location. In upstream rupture cases, the upstream segment showed significantly higher upstream radius gradient than the downstream segment. Conversely, in downstream rupture cases, the downstream radius gradient was significantly higher than the upstream segment.

FIGURE 5 Clinical Presentations According to Longitudinal Asymmetry of Lesion Geometry

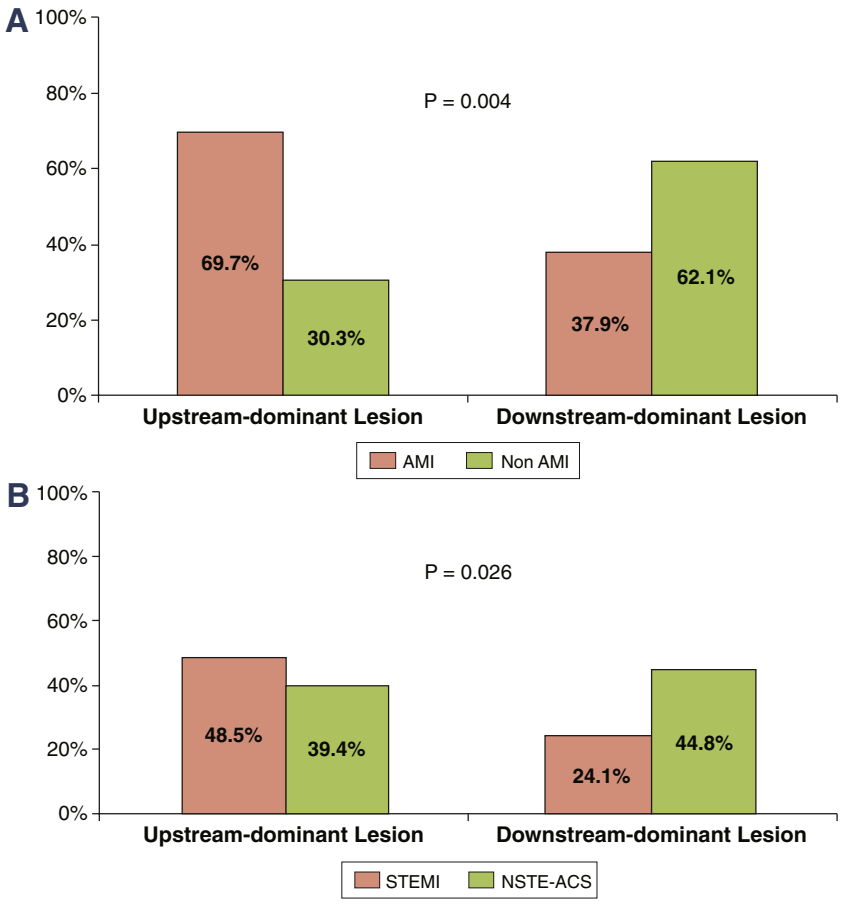

Clinical presentations were significantly different between upstream-dominant and downstream-dominant lesions. **(A)** Upstream-dominant cases more frequently manifested as acute myocardial infarction (AMI). **(B)** Frequency of ST-segment elevation myocardial infarction (STEMI) was also significantly different between upstream-dominant and downstream-dominant lesions. NSTE-ACS = non–ST-segment elevation acute coronary syndrome.

The risk of downstream rupture becomes lower in severe stenosis because the downstream APS decreases after a certain level of stenosis (>60% to 70% diameter stenosis in our study). The relatively lower incidence of STEMI and TIMI flow grade <3 in patients with lesions with downstream rupture may be explained by the relatively lower stenosis severity and less flow disturbance in such lesions.

STUDY LIMITATIONS. First, because this study included patients with clear rupture by IVUS, selection bias cannot be excluded. Second, RG could not be measured in plaques with MLA rupture because discrimination of definite MLA site was inherently impossible. Third, although we excluded patients with post-balloon angioplasty IVUS to avoid procedure-related rupture, the possibility of IVUS catheter-related plaque damage, especially in upstream segments, cannot be fully excluded. Fourth, diffuse lesions were excluded from the analysis. Given the complex geometry of those lesion subsets, RG cannot reliably represent longitudinal lesion asymmetry. Fifth, we focused on the hemodynamic and geometric parameters potentially related to plaque rupture, but we did not investigate the material properties of plaques (i.e., plaque vulnerability). Sixth, we could not fully evaluate segmental plaque composition or vulnerability parameters. Because the distribution of hemodynamic forces such as wall shear stress is determined by the interaction of blood flow and the surface of plaque, there can be a relationship between lesion geometry and plaque composition (7,37–40). Finally, the present study did not consider the abrupt change in physiological condition and the impact of mechanical

FIGURE 6 Association Between Lesion Geometry and Hemodynamic Force in Idealized Models

	Segmental Length		Radius			RG		% AS
	Upstream	Downstream	Upstream	MLA	Downstream	Upstream	Downstream	
Upstream-dominant	6.554	9.050	1.692	0.982	1.512	0.108	0.059	63.3%
Downstream-dominant	8.824	4.940	1.644	0.986	1.620	0.075	0.128	65.6%

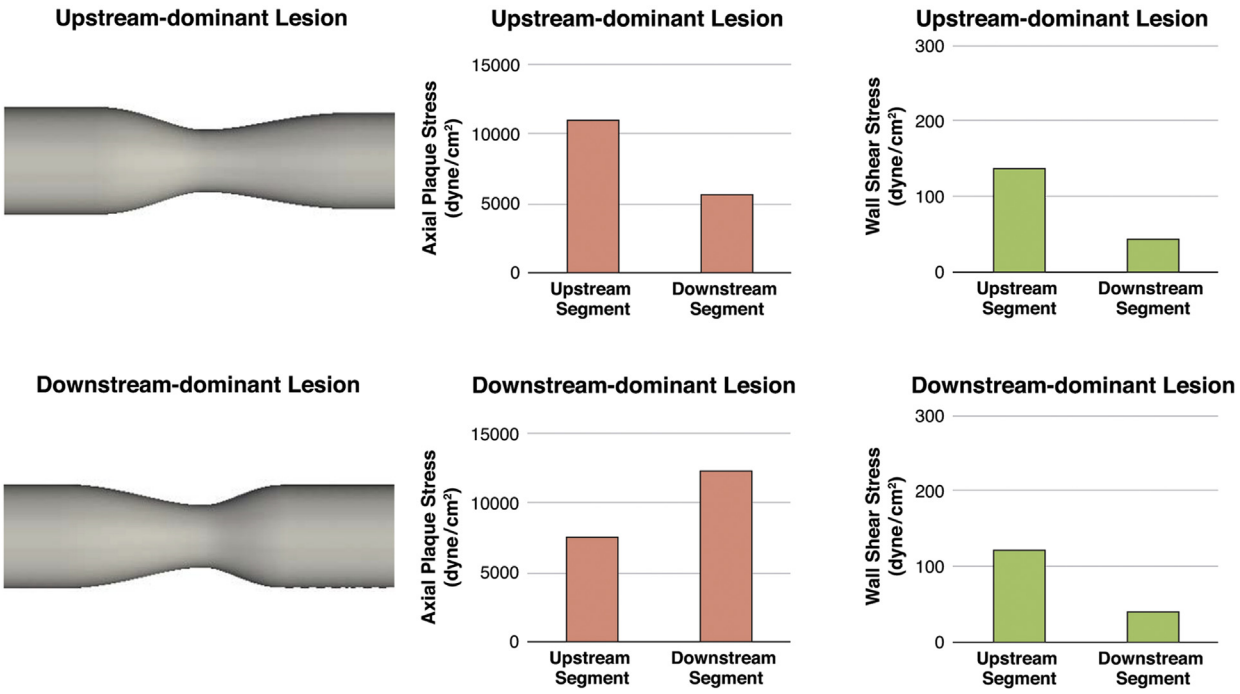

The idealized stenosis model was constructed using average values of intravascular ultrasound data from the study population. In upstream-dominant lesions (radius gradient $[RG]_{upstream} > RG_{downstream}$), axial plaque stress in the upstream segment was higher than in the downstream segment. The inverse was also true for downstream-dominant lesions ($RG_{upstream} < RG_{downstream}$). Conversely, wall shear stress predominated in upstream-segment lesions, regardless of longitudinal lesion geometry. In addition, the absolute magnitude of wall shear stress was significantly lower than that of axial plaque stress. AS = area stenosis; MLA = minimum lumen area.

stresses caused by cardiac contraction and relaxation. Further studies using fluid-structure interaction methods with incorporation of material properties and cardiac motion with dynamic changes in heart rate will provide a more comprehensive assessment for the risk of plaque rupture.

CONCLUSIONS

Clinical presentation and the degree of flow limitation were associated with the location of plaque rupture. Longitudinal lesion asymmetry assessed by RG, which can affect regional distribution of hemodynamic stress, was associated with the location of rupture, degree of flow limitation, and clinical presentation. Therefore, the concept of longitudinal lesion asymmetry or RG can be helpful in predicting the location and clinical consequence of plaque rupture in patients with coronary artery disease.

ACKNOWLEDGMENT The authors thank Mr. Dong-Jun Lee of Seoul National University Hospital for the analysis of IVUS images.

ADDRESS FOR CORRESPONDENCE: Dr. Bon-Kwon Koo, Department of Internal Medicine and Cardiovascular Center, Seoul National University Hospital, 101 Daehang-ro, Chongno-gu, Seoul 110-744, South Korea. E-mail: bkkoo@snu.ac.kr. OR Dr. Eun-Seok Shin, Department of Internal Medicine and Cardiovascular Center, Ulsan University Hospital, 290-3 Jeonha-dong, Dong-gu, Ulsan 682-714, South Korea. E-mail: ses@uuh.ulsan.kr OR sesim1989@gmail.com.

PERSPECTIVES

COMPETENCY IN MEDICAL KNOWLEDGE: Although plaque rupture is the main pathophysiological trigger for acute coronary syndrome, the relationships among lesion geometry, external hemodynamic forces acting on the plaque, location of plaque rupture, and clinical presentation have not been comprehensively investigated.

COMPETENCY IN PATIENT CARE AND PROCEDURAL SKILLS: Plaques rupture as a result of the complex interactions among intrinsic properties of individual plaque (vulnerability), extrinsic forces on plaque (trigger force), and strain within the plaque. Lesion geometry determines the distribution of hemodynamic forces that can act as a trigger force for plaque rupture and can influence the nature and constituents of the plaque itself. Therefore, assessment of lesion geometry may be helpful to understand the mechanism of rupture.

TRANSLATIONAL OUTLOOK 1: This study affirmed that patients with upstream plaque rupture showed a higher incidence of STEMI and TIMI flow grade <3 than did patients with downstream rupture or rupture at the MLA. The location of rupture was strongly associated with the longitudinal asymmetry of lesion geometry, which was assessed by RG (defined by the change in radius over the segmental lesion length). In patients with upstream or downstream segment rupture, the rupture was predominantly located in the segment of higher RG, and the RG ratio ($RG_{upstream}/RG_{downstream}$) was an independent predictor of rupture location.

TRANSLATIONAL OUTLOOK 2: CFD analysis demonstrated that APS was higher in locations with higher RG. Longitudinal lesion asymmetry assessed by RG, which can affect regional distribution of hemodynamic stress, was associated with the location of plaque rupture, the degree of flow limitation, and clinical presentation. Therefore, the concept of longitudinal lesion asymmetry or RG can be helpful in predicting the location and clinical consequences of plaque rupture in patients with coronary artery disease.

REFERENCES

1. Maehara A, Mintz GS, Bui AB, et al. Morphologic and angiographic features of coronary plaque rupture detected by intravascular ultrasound. J Am Coll Cardiol 2002;40:904–10.

2. Tanaka A, Shimada K, Namba M, et al. Relationship between longitudinal morphology of ruptured plaques and TIMI flow grade in acute coronary syndrome: a three-dimensional intravascular ultrasound imaging study. Eur Heart J 2008;29:38–44.

3. Lee CW, Hwang I, Park CS, et al. Comparison of intravascular ultrasound and histological findings in culprit coronary plaques between ST-segment elevation and non-ST-segment elevation myocardial infarction. Am J Cardiol 2013;112:68–72.

4. Shimamura K, Ino Y, Kubo T, et al. Difference of ruptured plaque morphology between asymptomatic coronary artery disease and non-ST elevation acute coronary syndrome patients: an optical coherence tomography study. Atherosclerosis 2014;235:532–7.

5. Takaoka N, Tsujita K, Kaikita K, et al. Comprehensive analysis of intravascular ultrasound and angiographic morphology of culprit lesions between ST-segment elevation myocardial infarction and non-ST-segment elevation acute coronary syndrome. Int J Cardiol 2014;171:423–30.

6. Dong L, Mintz GS, Witzenbichler B, et al. Comparison of plaque characteristics in narrowings with ST-elevation myocardial infarction (STEMI), non-STEMI/unstable angina pectoris and stable coronary artery disease (from the ADAPT-DES IVUS Substudy). Am J Cardiol 2015;115:860–6.

7. Kwak BR, Back M, Bochaton-Piallat ML, et al. Biomechanical factors in atherosclerosis: mechanisms and clinical implications. Eur Heart J 2014;35:3013–20, 3020a–d.

8. Choi G, Lee JM, Kim HJ, et al. Coronary artery axial plaque stress and its relationship with lesion geometry: application of computational fluid dynamics to coronary CT angiography. J Am Coll Cardiol Img 2015;8:1156–66.

9. TIMI IIIB Investigators. Effects of tissue plasminogen activator and a comparison of early invasive and conservative strategies in unstable angina and non-Q-wave myocardial infarction: results of the TIMI IIIB Trial. Thrombolysis in Myocardial Ischemia. Circulation 1994;89:1545–56.

10. Mintz GS, Nissen SE, Anderson WD, et al. American College of Cardiology clinical expert consensus document on standards for acquisition, measurement and reporting of intravascular ultrasound studies (IVUS): a report of the American College of Cardiology Task Force on Clinical Expert Consensus Documents. J Am Coll Cardiol 2001;37:1478–92.

11. Katritsis DG, Pantos J, Efstathopoulos E. Hemodynamic factors and atheromatic plaque rupture in the coronary arteries: from vulnerable plaque to vulnerable coronary segment. Coron Artery Dis 2007;18:229–37.

12. Pagiatakis C, Galaz R, Tardif JC, Mongrain R. A comparison between the principal stress direction and collagen fiber orientation in coronary atherosclerotic plaque fibrous caps. Med Biol Eng Comput 2015;53:545–55.

13. Doriot PA. Estimation of the supplementary axial wall stress generated at peak flow by an arterial stenosis. Phys Med Biol 2003;48:127–38.

14. Taylor CA, Fonte TA, Min JK. Computational fluid dynamics applied to cardiac computed tomography for noninvasive quantification of fractional flow reserve: scientific basis. J Am Coll Cardiol 2013;61:2233–41.

15. Naghavi M, Libby P, Falk E, et al. From vulnerable plaque to vulnerable patient: a call for new definitions and risk assessment strategies: part I. Circulation 2003;108:1664–72.

16. Niccoli G, Montone RA, Di Vito L, et al. Plaque rupture and intact fibrous cap assessed by optical coherence tomography portend different outcomes in patients with acute coronary syndrome. Eur Heart J 2015;36:1377–84.

17. Stone GW, Maehara A, Lansky AJ, et al. A prospective natural-history study of coronary atherosclerosis. N Engl J Med 2011;364:226–35.

18. Fujii K, Mintz GS, Carlier SG, et al. Intravascular ultrasound profile analysis of ruptured coronary plaques. Am J Cardiol 2006;98:429–35.

19. Imoto K, Hiro T, Fujii T, et al. Longitudinal structural determinants of atherosclerotic plaque vulnerability: a computational analysis of stress distribution using vessel models and three-dimensional intravascular ultrasound imaging. J Am Coll Cardiol 2005;46:1507–15.

20. Li ZY, Taviani V, Tang T, et al. The mechanical triggers of plaque rupture: shear stress vs pressure gradient. Br J Radiol 2009;82 Spec No 1:S39–45.

21. Otsuka F, Joner M, Prati F, Virmani R, Narula J. Clinical classification of plaque morphology in coronary disease. Nat Rev Cardiol 2014;11:379–89.

22. Fukumoto Y, Hiro T, Fujii T, et al. Localized elevation of shear stress is related to coronary plaque rupture: a 3-dimensional intravascular ultrasound study with in-vivo color mapping of shear stress distribution. J Am Coll Cardiol 2008;51:645–50.

23. Teng Z, Brown AJ, Calvert PA, et al. Coronary plaque structural stress is associated with plaque composition and subtype and higher in acute coronary syndrome: the BEACON I (Biomechanical Evaluation of Atheromatous Coronary Arteries) study. Circ Cardiovasc Imaging 2014;7:461–70.

24. Kusama I, Hibi K, Kosuge M, et al. Intravascular ultrasound assessment of the association between spatial orientation of ruptured coronary plaques and remodeling morphology of culprit plaques in ST-elevation acute myocardial infarction. Heart Vessels 2012;27:541–7.

25. von Birgelen C, Klinkhart W, Mintz GS, et al. Plaque distribution and vascular remodeling of ruptured and nonruptured coronary plaques in the same vessel: an intravascular ultrasound study in vivo. J Am Coll Cardiol 2001;37:1864–70.

26. Li ZY, Gillard JH. Plaque rupture: plaque stress, shear stress, and pressure drop. J Am Coll Cardiol 2008;52:1106–7; author reply 1107.

27. Narula J, Nakano M, Virmani R, et al. Histopathologic characteristics of atherosclerotic coronary disease and implications of the findings for the invasive and noninvasive detection of vulnerable plaques. J Am Coll Cardiol 2013;61:1041–51.

28. Calvert PA, Obaid DR, O'Sullivan M, et al. Association between IVUS findings and adverse outcomes in patients with coronary artery disease: the VIVA (VH-IVUS in Vulnerable Atherosclerosis) Study. J Am Coll Cardiol Img 2011;4:894–901.

29. Cheng JM, Garcia-Garcia HM, de Boer SP, et al. In vivo detection of high-risk coronary plaques by radiofrequency intravascular ultrasound and cardiovascular outcome: results of the ATHEROREMO-IVUS study. Eur Heart J 2014;35:639–47.

30. Vergallo R, Ren X, Yonetsu T, et al. Pancoronary plaque vulnerability in patients with acute coronary syndrome and ruptured culprit plaque: a 3-vessel optical coherence tomography study. Am Heart J 2014;167:59–67.

31. Inaba S, Mintz GS, Farhat NZ, et al. Impact of positive and negative lesion site remodeling on clinical outcomes: insights from PROSPECT. J Am Coll Cardiol Img 2014;7:70–8.

32. Xie Y, Mintz GS, Yang J, et al. Clinical outcome of nonculprit plaque ruptures in patients with acute coronary syndrome in the PROSPECT study. J Am Coll Cardiol Img 2014;7:397–405.

33. Kang SJ, Ahn JM, Han S, et al. Multimodality imaging of attenuated plaque using grayscale and virtual histology intravascular ultrasound and optical coherent tomography. Catheter Cardiovasc Interv 2016;88:E1–11.

34. Motoyama S, Ito H, Sarai M, et al. Plaque characterization by coronary computed tomography angiography and the likelihood of acute coronary events in mid-term follow-up. J Am Coll Cardiol 2015;66:337–46.

35. Motoyama S, Sarai M, Harigaya H, et al. Computed tomographic angiography characteristics of atherosclerotic plaques subsequently resulting in acute coronary syndrome. J Am Coll Cardiol 2009;54:49–57.

36. Madder RD, Goldstein JA, Madden SP, et al. Detection by near-infrared spectroscopy of large lipid core plaques at culprit sites in patients with acute ST-segment elevation myocardial infarction. J Am Coll Cardiol Intv 2013;6:838–46.

37. Malek AM, Alper SL, Izumo S. Hemodynamic shear stress and its role in atherosclerosis. JAMA 1999;282:2035–42.

38. Langille BL, O'Donnell F. Reductions in arterial diameter produced by chronic decreases in blood flow are endothelium-dependent. Science 1986;231:405–7.

39. Stone PH, Saito S, Takahashi S, et al. Prediction of progression of coronary artery disease and clinical outcomes using vascular profiling of endothelial shear stress and arterial plaque characteristics: the PREDICTION Study. Circulation 2012;126:172–81.

40. Chatzizisis YS, Coskun AU, Jonas M, Edelman ER, Feldman CL, Stone PH. Role of endothelial shear stress in the natural history of coronary atherosclerosis and vascular remodeling: molecular, cellular, and vascular behavior. J Am Coll Cardiol 2007;49:2379–93.

KEY WORDS computational fluid dynamics, coronary plaque, intravascular ultrasound, myocardial infarction, plaque rupture

APPENDIX For an expanded methods section as well as a supplemental table and figures, please see the online version of this article.